



## Materials Performance and Characterization

---

O. O. Joseph,<sup>1</sup> C. A. Loto,<sup>2</sup> J. Ade Ajayi,<sup>3</sup> S. Sivaprasad<sup>4</sup>

**DOI: 10.1520/MPC20160011**

Role of Chloride on the  
Environmental  
Degradation of  
Micro-Alloyed Steel in  
Simulated Fuel Grade  
Ethanol Environment

---

VOL. 6 / NO. 3 / 2017

O. O. Joseph,<sup>1</sup> C. A. Loto,<sup>2</sup> J. Ade Ajayi,<sup>3</sup> S. Sivaprasad<sup>4</sup>

## Role of Chloride on the Environmental Degradation of Micro-Alloyed Steel in Simulated Fuel Grade Ethanol Environment

### Reference

Joseph, O. O., Loto, C. A., Ade Ajayi, J., Sivaprasad, S., "Role of Chloride on the Environmental Degradation of Micro-Alloyed Steel in Simulated Fuel Grade Ethanol Environment," *Materials Performance and Characterization*, Vol. 6, No. 3, 2017, pp. 334-345, <http://dx.doi.org/10.1520/MPC20160011>. ISSN 2165-3992

Manuscript received February 18, 2016; accepted for publication October 11, 2016; published online April 12, 2017.

<sup>1</sup> Dept. of Mechanical Engineering, Covenant Univ., P.M.B. 1023, Canaanland, Ota, Nigeria (Corresponding author), e-mail: [funmi.joseph@covenantuniversity.edu.ng](mailto:funmi.joseph@covenantuniversity.edu.ng)

<sup>2</sup> Dept. of Mechanical Engineering, Covenant Univ., P.M.B. 1023, Canaanland, Ota, Nigeria

<sup>3</sup> Department of Metallurgical and Materials Engineering, Federal University of Technology, P.M.B. 704, Akure, Nigeria

<sup>4</sup> Materials Science and Technology Division, CSIR-National Metallurgical Laboratory, 831007, Jamshedpur, India

### ABSTRACT

In this study, micro-alloyed steel (MAS) material commonly used in the manufacture of auto parts and pipes was immersed in simulated fuel grade ethanol (SFGE) blends and its performance was evaluated. In order to determine the role of chloride on corrosion behavior, electrochemical measurement was conducted in low-conductivity ethanolic solutions in the absence of supporting electrolyte; also mass loss test was performed. Consistent with the mass loss and electrochemical test results, the effect of chloride on the degradation of MAS in the fuel ethanol environments can be classified from the least corrosive concentration to the highest as follows:  $0 \text{ mg/L} < 32 \text{ mg/L} < 64 \text{ mg/L NaCl}$ . Chloride increased the pitting tendency of MAS in E20, E40, and E80 blends.

### Keywords

micro-alloyed steel, fuel-grade ethanol, polarization, chloride, pitting

## Introduction

Over the last ten years, many governments have commenced looking for a way to combat the impact of fuel emissions on the environment. Consequently, the use of fuel ethanol by blending it with gasoline has become prevalent in a number of countries. In so doing, fewer emissions are released into the environment, contributing significantly to greenhouse gas (GHG) mitigation. E10 (10 % bioethanol – 90 % gasoline), which is one of the most prevalent biofuel blends, is used as a substitute for gasoline. Ethanol is one of the core components of impending reformulated fuels and suggests limitless advantages due to its physical and chemical characteristics, low production costs, and environmental friendliness, amongst many others [1]. Such advantages include a thriving farm industry, reduced dependence on foreign oil, lower emissions, and valuable use of by-products. However, fuel ethanol has some downsides regarding material compatibility. Its chemical composition can have a degrading effect on materials that are typically compatible with gasoline [2–4].

Incidents of corrosion attack have been found in some fuel ethanol system materials such as castings in fuel pumps and fuel tanks, steel, and aluminum alloys [1,5]. The presence of components such as chlorides, water, methanol, dissolved oxygen, and acetic acid within the established limits by the American Society for Testing and Materials (ASTM) in ASTM D4806-16a [6] might increase the susceptibility of steel to corrosion and stress corrosion cracking (SCC) [7]. When dissolved oxygen was minimized through nitrogen purging, there was no SCC in the presence of all additional species at their maximum levels. However, on introducing oxygen, SCC occurred [7]. In addition, a study carried out by the American Petroleum Institute [8] involved the use of corrosion potential technique for evaluating SCC susceptibility of steel when exposed to ethanol. The results revealed increased proneness to SCC with increasing corrosion potential. Further studies include the addition of chemical additives to SFGE to provide scavenging of oxygen in solution as well as inhibition of SCC in fuel grade ethanol (FGE) using slow strain rate (SSR) techniques [9], besides examination of pitting corrosion in SFGE solutions on carbon steel [10]. The results obtained by scavenging oxygen showed a dependence of ethanol SCC on corrosion potential that was consistent with observations from previous American Petroleum Institute (API) studies.

The effect of inorganic chloride in ethanolic solutions on the SCC behavior of carbon steels has also been investigated by varying the inorganic chloride concentrations between 0 and 70 mg/L [11], and a much wider concentration from 0 to 0.1 M [12] in SFGE. Lou et al. [11] reported that chloride disrupts surface film and enhances pitting corrosion. Cao et al. [12] found that chloride is required for ethanol SCC but is not the governing influence for crack growth. Besides, significant information has been collected from reviews, reports, and summaries of studies investigating the compatibility of fuel ethanol with certain metallic materials [13–15]. All of the findings point to the fact that SCC of metals do occur in fuel grade ethanol (FGE) environment, whether simulated or field FGE due to several factors that have been mentioned.

In this study, micro-alloyed steel is analyzed for failure in simulated E20, E40, and E80 fuel ethanol environments under aerated conditions. Micro-alloyed steel is

**TABLE 1**

Chemical composition of micro-alloyed steel in as-received condition.

Element	C	Mn	Si	Cr	Ni	Al	Ti	Mo	Cu	Fe
Micro-alloyed	0.13	0.77	0.012	0.027	0.015	0.042	0.0025	0.0017	0.006	balance

a cost-effective high strength steel, which has favorable application in the automotive industry. Nonetheless, there is sparse information in literature regarding the corrosion behavior of micro-alloyed steel in fuel ethanol blends.

## Experimental

### MATERIALS AND TEST ENVIRONMENTS

The metal specimens used for this study were machined from new micro-alloyed steel plates in as-received condition. The chemical composition of this steel is presented in **Table 1**. The fuels used for immersion and electrochemical tests were E20, E40, and E80 blends. The simulated fuel ethanol test environments were prepared partly in consistence with ASTM Standard D4806 [6] for fuel grade ethanol. The reagents used include: 195 proof ethanol, glacial acetic acid, pure methanol, pure sodium chloride (NaCl) with purity >99 %, and ultra-pure water (~18 MΩ·cm). NaCl was first dissolved in water, and then added to ethanol to reach the specified NaCl and water concentrations, respectively, for each of the fuel blends. The concentration of chloride was methodically altered to study its influence on the corrosion and fracture behavior of micro-alloyed steel. This was achieved by using 0, 32, and 64 mg/L chloride ion (Cl<sup>-</sup>) concentrations [16]. The denaturant used was unleaded gasoline. The baseline composition for the simulated fuel-grade ethanol used in this study is shown in **Table 2**. All reagents used were of analytical grade. The corrosion tests were carried out in aerated conditions at room temperature of 27°C. To study the influence of chloride, reference tests were carried out in the absence of chloride for all the ethanol concentrations.

### IMMERSION TEST

Flat square coupons of dimensions 30 by 30 by 11 mm were machined from micro-alloyed steel plates for mass loss tests. The specimens were dry-abraded up to 800 grit, degreased with acetone, and used immediately for testing. The area as well as weight of each specimen was measured before exposure to the test environments for the purpose of post-calculation. Immersion of duplicate samples for each test condition was carried out for 60 days' duration. A total of 18 samples were used for the test. Each sample was suspended in 300 ml of the test solution using airtight plastic containers. For E20 blend, the test solution of 300 ml was obtained by adding 240 ml unleaded gasoline to 60 ml SFGE. E40 and E80 blends were also prepared by the

**TABLE 2**

Baseline composition of simulated fuel grade ethanol used for the tests.

195 Proof Ethanol (vol. %)	Methanol (vol. %)	Water (vol. %)	NaCl (mg/L)	Acetic Acid (mg/L)
98.5	0.5	1	32	56

addition of 180 ml unleaded gasoline to 120 ml SFGE and 60 ml unleaded gasoline to 240 ml SFGE, respectively. The solution was replenished fortnightly to diminish changes in solution composition, replace the ionic impurities, and to compensate for evaporation. After the immersion tests, thick oxide films formed on the samples' surfaces were removed by mechanical and chemical means, in accordance with ASTM G1-03(2011) [17] for preparing, cleaning, and evaluating corrosion test specimens. The surfaces of the corroded samples were further characterized using a FEI-430 NOVA NANO FEG-SEM and a Jeol scanning electron microscope.

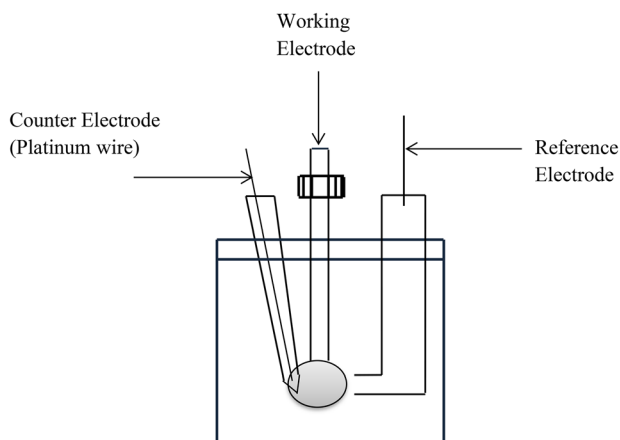
### ELECTROCHEMICAL MEASUREMENTS

A Gamry reference 600 Potentiostat/Galvanostat/ZRA was used for open circuit potential (OCP) and anodic polarization measurements. The test setup comprises of a three electrode glass cell with saturated calomel electrode (SCE) as the reference electrode and platinum electrode as a counter electrode (**Fig. 1**).

The platinum electrode was constructed by using a glass frit to isolate platinum wire from the working electrode. To minimize the effect of high solution resistance associated with ethanolic solutions [12,18], the electrochemical cell was designed in such a way as to ensure minimal distance between the working electrode and the lugin capillary of the reference electrode. Each experiment was carried out in duplicate so as to determine the reproducibility of the experiments. Eighteen rectangular samples with dimensions 14 by 10 by 5 mm were used for the electrochemical tests. The samples were dry-abraded up to 2000 grit, degreased with acetone, and dried. The test samples were further mounted with bakelite, in this manner decreasing contact area. The mounted samples were threaded to a carbon steel rod (working electrode) and suspended in solution. The working electrode was also insulated from the test solution by means of a Teflon<sup>®</sup> tape. All the polarization tests began with cathodic polarization at  $-0.75$  V versus SCE in order to ensure similar reduced metal surfaces for the tests. A potential scan rate of 2 mV/s was used to lessen the influence of chloride leakage from high-silica glass as described elsewhere [9,18].

**FIG. 1**

Schematic of the electrochemical cell design for anodic polarization tests.



### VISUAL EXAMINATION AND DETERMINATION OF CORROSION RATES

Visual examination was carried out to verify existence of pits, discoloration at the completion of exposure, or alteration of surface texture. Weight measurements were taken to record the mass loss of each specimen exposed to the test environment. The corrosion rate was computed in mils per year (mpy) using equation (1) in accordance with ASTM Standard G1-03 [17]:

$$\text{Corrosion rate} = (K \times W)/(A \times T \times D) \quad (1)$$

where:

- $K$  = a constant (534),
- $T$  = the exposure time in hours,
- $A$  = the sample area in square inches,
- $W$  is the mass loss in milligrams, and
- $D$  is the density in  $\text{g}/\text{cm}^3$ .

### MICROSTRUCTURE AND RAMAN SPECTROSCOPY ANALYSIS

Characterization of surface morphology after corrosion was carried out using a FEG-SEM, coupled with energy dispersive spectrometer (EDS). The corrosion products from immersion tests were analyzed with Nicolet Almega XR Dispersive Raman spectrometer having a wavelength of 530 nm.

## Results and Discussion

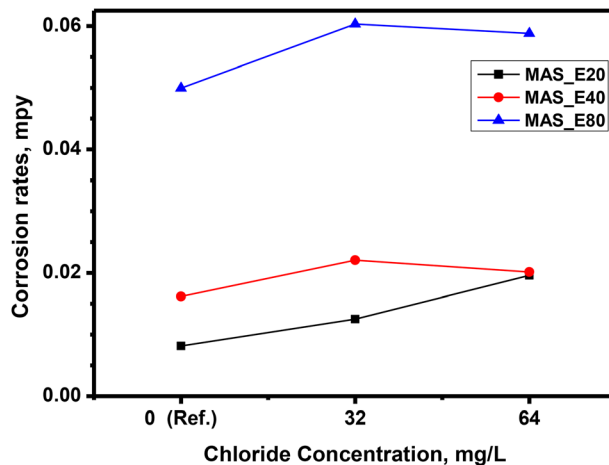
### ROLE OF CHLORIDE ON MASS LOSS TESTS

For each ethanol concentration, the effect of chloride was investigated via 32 and 64 mg/L NaCl and with respect to a reference test in the absence of chloride. The effect of NaCl additions on the corrosion behaviour of micro-alloyed steel in E20, E40 and E80 is shown in Fig. 2.

In E20, corrosion rate is seen to increase from  $8.17\text{E}-03$  mpy in the absence of chloride to  $1.25\text{E}-02$  mpy upon addition of 32 mg/L chloride concentration. When

**FIG. 2**

Effect of chloride on the corrosion rate of MAS in simulated E20, E40 and E80 fuel ethanol environments (average values).



chloride was increased to 64 mg/L, a higher corrosion rate of 1.96E-02 mpy was observed. This implies that with chloride addition and increasing chloride concentration, the material deteriorates in E20 with respect to the reference test in the absence of chloride. Similarly, in both E40 and E80 with 32 mg/L NaCl, there was increase in corrosion rate with respect to the reference test from 1.62E-02 to 2.21E-02 mpy in E40 and 4.99E-02 to 6.03E-02 mpy in E80. However, the addition of 64 mg/L NaCl caused a drop in corrosion rate of MAS in E40 (2.01E-02 mpy) and E80 (5.88E-02 mpy). This behaviour was unexpected as chloride products formed are not expected to improve corrosion behaviour [19].

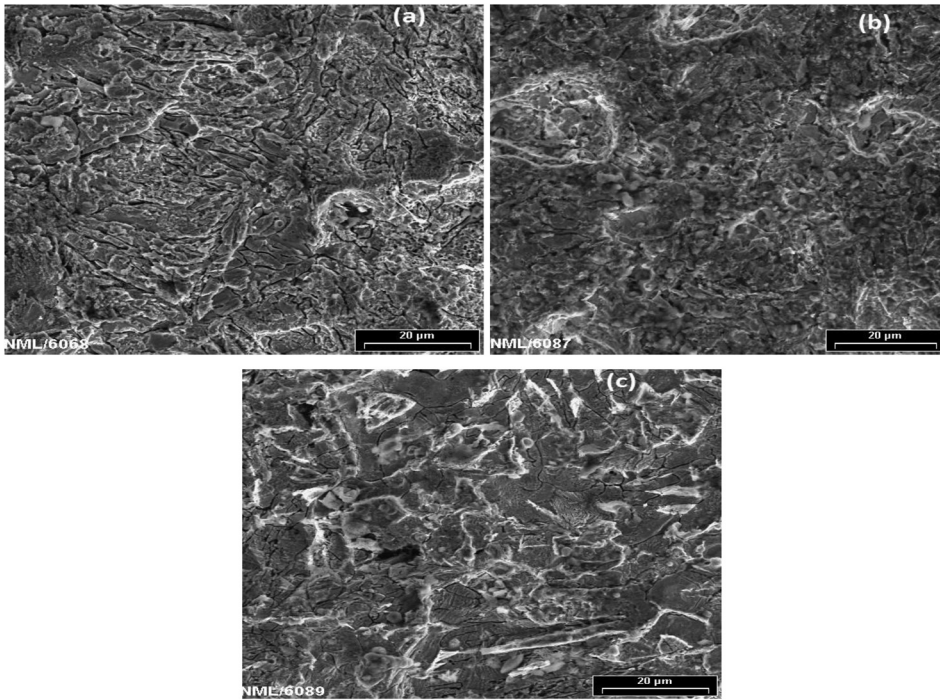
Generally, the presence of chloride ions in solution initiates breakdown of passivity and the reaction is known to be diffusion controlled. Nevertheless, in sodium chloride solutions at certain concentrations (dependent on material-environment system), the film thickening rate can increase with increasing concentration of sodium chloride [20,21]. In this work, the adsorption of chloride ions in micro-alloyed steel, up to a threshold concentration of 32 mg/L from E40 and E80 fuel ethanol environments, resulted in degradation of the material. At higher chloride concentration of 64 mg/L, corrosive actions at the grain boundaries have been slowed down, thereby reducing corrosion rate. The margin of reduction in corrosion rate of MAS in E40 and E80 in the presence of 64 mg/L NaCl is very small, approximately 9 % in the case of E40 and 2 % in the case of E80. Consequently, the low margin of reduction suggests that increasing chloride concentration does not have any significant effect on the corrosion rate of MAS in E40 and E80 simulated fuel ethanol blends. However, an assessment of all the test conditions reveals that, the reference test carried out in the absence of chloride, displays the lowest corrosion rate. Therefore, the presence of chloride in fuel ethanol either in low or high concentrations can be said to be a potential problem in the life cycle of MAS.

**Figs. 3–5** show the morphology of MAS samples after 60 days of immersion in the presence and absence of chloride, taken at identical magnification of 1000x. Pitting (localized) corrosion is obvious on the SEM images of the samples, which were immersed in E20, E40, and E80 with 32 mg/L NaCl (**Fig. 4**). The existence of pits is attributed to the action of chloride since no pitting was detected on the samples tested in the absence of chloride. This finding is in agreement with published literature regarding the role of chloride on corrosion of carbon steel in simulated fuel grade ethanol environment [18]. It must also be pointed out that for micro-alloyed steel samples immersed in E20, both pit size and pit density increased as chloride concentration increased from 32 to 64 mg/L as shown by the SEM images in **Fig. 5**.

### ROLE OF CHLORIDE ON ELECTROCHEMICAL TESTS

Anodic polarization was used to investigate the polarization behavior of MAS. Reference electrochemical tests were carried out in the absence of chloride and used as a basis for investigating the effect of chloride on polarization behavior of MAS. The effects of chloride and increasing chloride concentration on the polarization behavior of MAS in the presence and absence of chloride are shown in **Fig. 6**. In order to mimic a parallel outcome of potential disruption from equilibrium in the fuel ethanol environments, MAS samples were anodically polarized with identical potential difference (1.5V<sub>SCE</sub>) from their preliminary OCPs. The result in **Fig. 6** shows that MAS does not exhibit distinct passivation behavior as well as pitting potential with

**FIG. 3** Post-corrosion SEM images of MAS at 1000x after 60 days immersion in (a) E20, (b) E40, and (c) E80 in the absence of NaCl showing presence of cracks and absence of pits.



anodic polarization in the range of ethanol-chloride ratio. Poor passivity was exhibited by MAS in the fuel ethanol environments, which is consistent with the behavior of metals in alcoholic environments as reported in literature [18]. To permit a number of corrosion kinetics and elimination of chloride seepage from the salt bridge, the polarization experiments were carried out at a scan rate of 2 mV/s. The  $E_{corr}$  and  $i_{corr-estimate}$  as observed for each test condition are shown in **Table 3**. For all the samples tested in E20, E40, and E80, the evaluated current density ( $I_{corr-estimate}$ )

**FIG. 4** Post-corrosion SEM images of MAS at 500x after 60 days immersion in (a) E40 and (b) E80 with additions of 32 mg/L NaCl showing pitting due to presence of chloride.

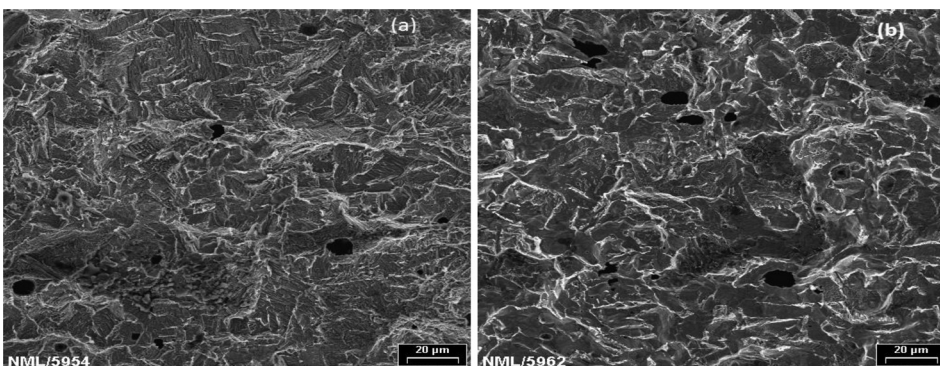
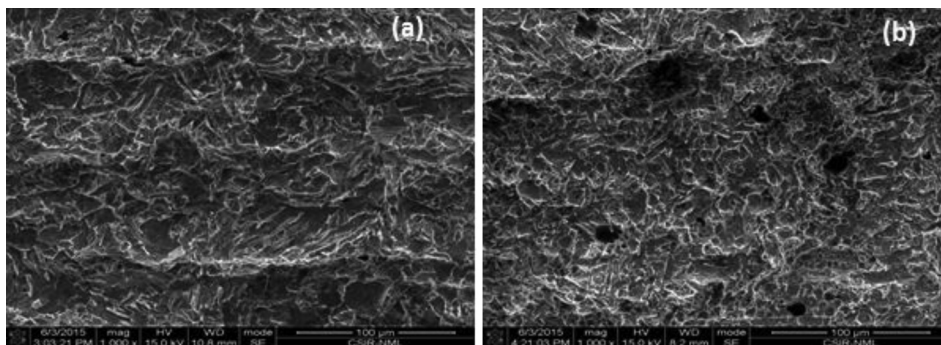


**FIG. 5** Post-corrosion SEM images of MAS at 1000x after 60 days immersion in E20 with additions of (a) 32 mg/L NaCl showing few pits, and (b) 32 mg/L NaCl showing increase in diameter and density of pits.



measured from the polarization curves increased with increasing chloride concentration up to 64 mg/L chloride. It is important to state that the corrosion rates obtained by immersion tests in E40 and E80 do not entirely agree with the polarization test results. From the mass loss tests, a decrease in corrosion rate of MAS was observed with 64 mg/L chloride concentration in E40 and E80. The poor correlation seen between the 60 days' mass loss corrosion rates and the electrochemical corrosion rates is probably caused by the protective action of thick corrosion products formed on the samples with longer exposure time during the mass loss tests. The polarization measurement gave a picture of the corrosion rate, while the mass loss measurement integrated the corrosion rate over the time of immersion.

However, consistent with the mass loss and electrochemical test results, the effect of chloride on the degradation of MAS in the fuel ethanol environments can be classified from the least corrosive concentration to the highest as follows: 0 mg/L < 32 mg/L < 64 mg/L NaCl.

#### **CHARACTERIZATION OF THE OXIDE LAYERS FORMED ON MAS EXPOSED TO E20, E40, AND E80**

Analyses of the corroded steels after 60 days of immersion in E20, E40, and E80 at 27°C were carried out by Raman spectroscopy. **Fig. 7** shows the results of Raman spectroscopy of the corrosion products. It reveals the presence of iron oxyhydroxides such as iron hydroxide [Fe(OH)<sub>2</sub>], goethite [ $\alpha$ -FeOOH], and maghemite [ $\gamma$ -Fe<sub>2</sub>O<sub>3</sub>] [22–24]. A strong band at 549 cm<sup>-1</sup> is found, signifying the presence of hematite. The existence of water in the simulated fuel ethanol environments stimulates the formation of iron hydroxide as reported elsewhere [18]. A broad and stronger band at 1423 cm<sup>-1</sup> present in the Raman spectroscopy of corrosion products obtained from samples immersed in the presence and absence of NaCl indicates the presence of maghemite. A strong band of Goethite is also present at 550 cm<sup>-1</sup>.

## **Conclusion**

The role of chloride in the environmental degradation of micro-alloyed steel in simulated E20, E40, and E80 fuel ethanol blends has been studied with 0–64 mg/L NaCl concentration. The specific conclusions arrived at are as follows:

**FIG. 6**

Effect of chloride on anodic polarization of MAS in (a) E20, (b) E40, and (c) E80 showing lower current density measured for MAS in E20 in all the tested conditions.

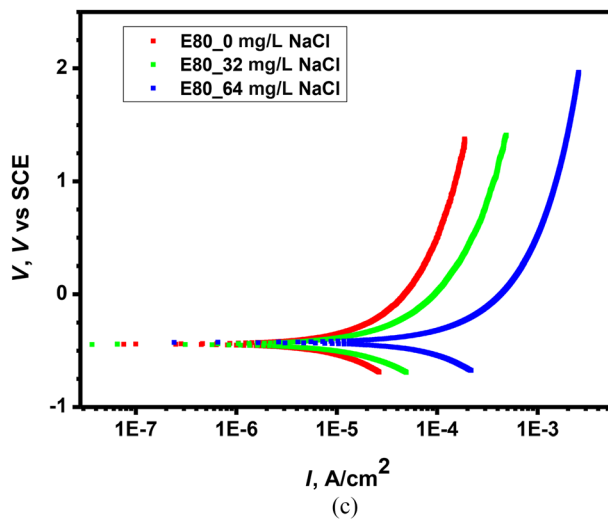
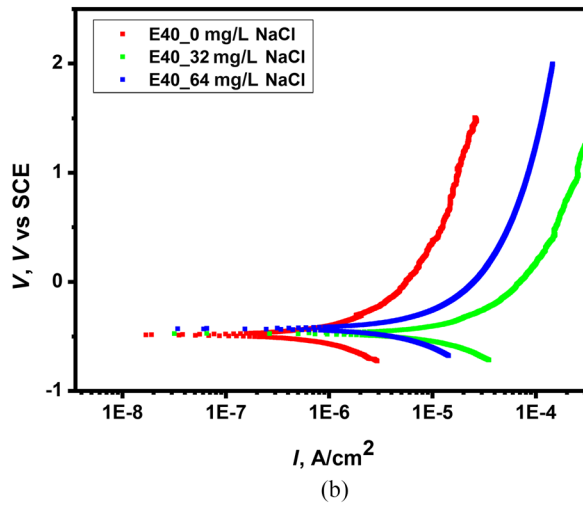
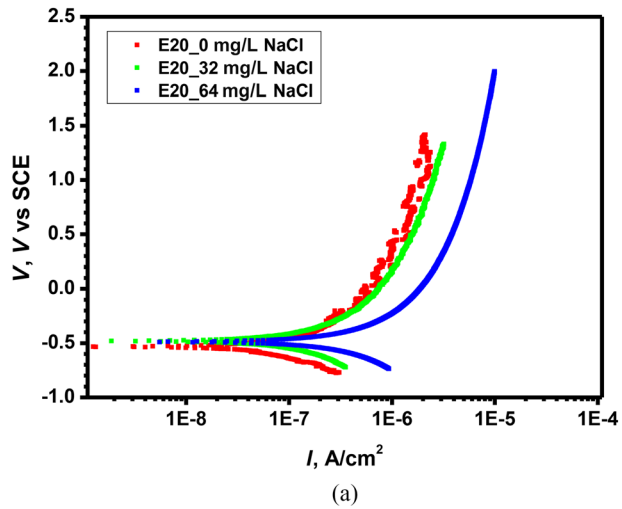


**TABLE 3**

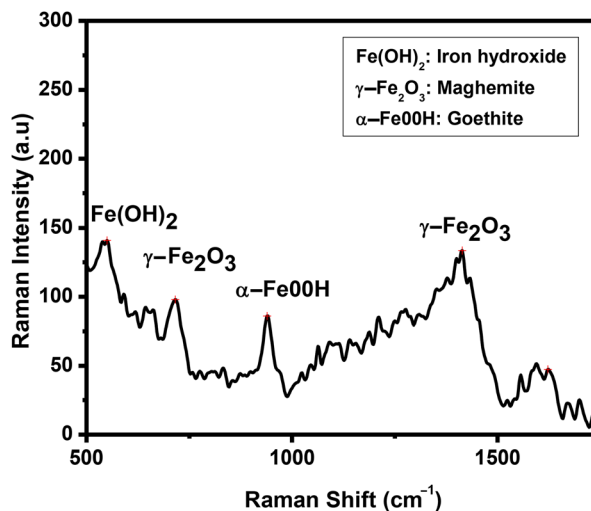
Anodic polarization data showing the influence of chloride in E20, E40, and E80 environments.

Test Environment	$E_{corr}$ (mV)	$i_{corr-estimate}$ (A/cm <sup>2</sup> )	CR (mpy)
E20 + 0 mg/L NaCl	-4.45E+02	4.64E-07	2.07E-01
E20 + 32 mg/L NaCl	-4.40E+02	2.41E-06	1.07E+00
E20 + 64 mg/L NaCl	-4.73E+02	7.14E-06	3.18E+00
E40 + 0 mg/L NaCl	-4.86E+02	1.73E-05	7.73E+00
E40 + 32 mg/L NaCl	-4.19E+02	1.87E-05	8.33E+00
E40 + 64 mg/L NaCl	-4.40E+02	5.51E-05	2.46E+01
E80 + 0 mg/L NaCl	-3.93E+02	7.99E-05	3.56E+01
E80 + 32 mg/L NaCl	-4.13E+02	8.27E-05	3.69E+01
E80 + 64 mg/L NaCl	-4.27E+02	9.92E-05	4.42E+01

1. Chloride increased the pitting tendency of MAS in E20, E40, and E80 blends. In the absence of chloride, no pitting was observed.
2. The mass loss of MAS increased in E20 with increase in chloride concentration up to 64 mg/L.
3. In E40 and E80, mass loss of MAS increased with the presence of chloride up to a concentration of 32 mg/L; beyond that threshold, the effect of increasing chloride was insignificant.
4. The correlation between mass loss corrosion rates and electrochemical corrosion rates is poor. The lack of agreement is probably caused by the protective action of thick corrosion products formed on the samples with longer exposure time during the mass loss tests.
5. Consistent with the mass loss and electrochemical test results, the effect of chloride on the degradation of MAS in the fuel ethanol environments can be classified from the least corrosive concentration to the highest as follows: 0 mg/L < 32 mg/L < 64 mg/L NaCl.

**FIG. 7**

Raman shift of corrosion products from MAS in simulated fuel ethanol showing the presence of iron hydroxide, maghemite, and goethite.



### ACKNOWLEDGMENTS

This work was sponsored by CSIR-National Metallurgical Laboratory, Jamshedpur, India and Third World Academy of Sciences (TWAS), Trieste, Italy in collaboration with Covenant University, Ota, Nigeria under the CSIR-TWAS Postgraduate fellowship scheme (FR No. 3240275047).

### References

- [1] Baena, L. M., Gomez, M., and Calderon, J. A., "Aggressiveness of a 20 % Bioethanol-80 % Gasoline Mixture on Autoparts: I Behaviour of Metallic Materials and Evaluation of Their Electrochemical Properties," *Fuel*, Vol. 95, 2012, pp. 320–328, <http://dx.doi.org/10.1016/j.fuel.2011.12.002>
- [2] Owen, K. and Coley, T., *Automotive Fuels Handbook*, Society of Automotive Engineers, Warrendale, PA, 1990.
- [3] Kane, R. D. and Maldonado, J. G., "Stress Corrosion Cracking of Carbon Steel in Fuel Grade Ethanol: Review and Survey," *API Technical Report 939-D*, American Petroleum Institute, Washington, D.C., 2003.
- [4] Kane, R. D., Sridhar, N., Brongers, M., Beavers, J. A., Agarwal, A. K., and Klein, L., "Stress Corrosion Cracking in Fuel Ethanol: A Recently Recognized Phenomenon," *Mater. Perform.*, Vol. 44, No. 12, 2005, pp. 50–55.
- [5] De Souza, J. P., Mattos, O. R., Sathler, L., and Takenouti, H., "Impedance Measurements of Corroding Mild Steel in an Automotive Fuel Ethanol With and Without Inhibitor in a Two and Three Electrode Cell," *Corros. Sci.*, Vol. 27, 1987, pp. 1351–1364, [http://dx.doi.org/10.1016/0010-938X\(87\)90130-2](http://dx.doi.org/10.1016/0010-938X(87)90130-2)
- [6] ASTM D4806-16a, *Standard Specification for Denatured Fuel Ethanol for Blending with Gasolines for Use as Automotive Spark-Ignition Engine Fuel*, ASTM International, West Conshohocken, PA, 2016, [www.astm.org](http://www.astm.org)
- [7] Pedraza-Basulto, G. K., Arizmendi-Morquecho, A. M., Cabral Miramontes, J. A., Borunda-Terrazas, A., Martinez-Villafane, A., and Chacon-Nava, J. G., "Effect of Water on the Stress Corrosion Cracking Behaviour of API 5L-X52 Steel in E95 Blend," *Int. J. Electrochem. Sci.*, Vol. 8, 2013, pp. 5421–5437, <http://www.electrochemsci.org/papers/vol8/80405421.pdf>
- [8] API, "Stress Corrosion Cracking of Carbon Steel in Fuel-Grade Ethanol: Review, Experience Survey, Field Monitoring and Laboratory Testing," *API Technical Report 939-D*, 2nd ed., American Petroleum Institute, Washington, D.C., 2007.
- [9] Lou, X., Yang, D., and Singh, P. M., "Effect of Ethanol Chemistry on Stress Corrosion Cracking of Carbon Steel in Fuel-Grade Ethanol," *Corrosion*, Vol. 65, No. 12, 2009, pp. 785–797, <http://dx.doi.org/10.5006/1.3319105>
- [10] Beavers, J. A., Brongers, M. P., Agrawal, A. K., and Tallarida, F. A., "Prevention of Internal SCC in Ethanol Pipelines," presented at *Corrosion 2008*, New Orleans, LA, March 16–20, 2008, NACE International, Houston, TX—unpublished.
- [11] Lou, X., Yang, D., Goodman, R. L., and Singh, P. M., "Understanding the Stress Corrosion Cracking of X-65 Pipeline Steel in Fuel Grade Ethanol," presented at *Corrosion 2010*, San Antonio, TX, March 14–18, 2010, NACE International, Houston, TX—unpublished.

- [12] Cao, L., Frankel, G. S., and Sridhar, N., "Effect of Chloride on Stress Corrosion Cracking Susceptibility of Carbon Steel in Simulated Fuel Grade Ethanol," *Electrochim. Acta*, Vol. 104, 2013, pp. 255–266, <http://dx.doi.org/10.1016/j.electacta.2013.04.112>
- [13] QINETIQ, *Assessing Compatibility of Fuel Systems with Bio-Ethanol and the Risk of Carburetor Icing*. U.K. Department for Transport, 2010. Retrieved from [www.realclassic.co.uk/techfiles/bioethanol\\_fuel\\_study.pdf](http://www.realclassic.co.uk/techfiles/bioethanol_fuel_study.pdf) (accessed October 29, 2010).
- [14] Concawe, "Guidelines for Handling and Blending Motor Gasoline Containing up to 10 % v/v Ethanol," *Report No. 3/08*, Special Task Force, FE/STF-24, Brussels, Belgium, 2008.
- [15] Minnesota Pollution Control Agency, *E20: The Feasibility of 20 Percent Ethanol Blends by Volume as a Motor Fuel, Executive Summary Results of Materials Compatibility and Drivability Testing*, St. Paul, MN, 2008.
- [16] Joseph, O. O., Loto, C. A., Sivaprasad, S., Ajayi, J. A., and Tarafder, S., "Role of Chloride in the Corrosion and Fracture Behaviour of Micro-Alloyed Steel in E80 Simulated Fuel Grade Ethanol Environment," *Materials*, Vol. 9, No. 6, 2016, p. 463, <http://dx.doi.org/10.3390/ma9060463>
- [17] ASTM G1-03(2011), *Standard Practice for Preparing, Cleaning and Evaluating Corrosion Test Specimens*, ASTM International, West Conshohocken, PA, 2011, [www.astm.org](http://www.astm.org)
- [18] Lou, X. and Singh, P. M., "Role of Water, Acetic Acid and Chloride on Corrosion and Pitting Behaviour of Carbon Steel in Fuel-Grade Ethanol," *Corros. Sci.*, Vol. 52, No. 7, 2010, pp. 2303–2315, <http://dx.doi.org/10.1016/j.corsci.2010.03.034>
- [19] Brown, K. R. and Baratta, F. I., eds., *Chevron-Notch Fracture Test Experience: Metals and Non-Metals*, ASTM STP 1172, ASTM International, West Conshohocken, PA, 1992.
- [20] Desouky, H. E. and Aboeldahab, H. A., "Effect of Chloride Concentration on the Corrosion Rate of Maraging Steel," *Open J. Phy. Chem.*, Vol. 4, No. 4, 2014, pp. 147–165, <http://dx.doi.org/10.4236/ojpc.2014.44018>
- [21] Roman, J., Vera, R., Bagnara, M., Carvajal, A. M., and Aperador, W., "Effect of Chloride Ions on the Corrosion of Galvanized Steel Embedded in Concrete Prepared With Cements of Different Composition," *Int. J. Electrochem. Sci.*, Vol. 9, No. 2, 2014, pp. 580–592.
- [22] Hanesch, M., "Raman Spectroscopy of Iron Oxides and (Oxy) Hydroxides at Low Laser Power and Possible Applications in Environmental Magnetic Studies," *Int. J. Geophys.*, Vol. 177, No. 3, 2009, pp. 941–948, <http://dx.doi.org/10.1111/j.1365-246X.2009.04122.x>
- [23] Oh, S. J., Cook, D. C., and Townsend, H. E., "Characterization of Iron Oxides Commonly Formed as Corrosion Products on Steel," *Hyperfine Interact.*, Vol. 112, No. 1, 1998, pp. 59–66, <http://dx.doi.org/10.1023/A:1011076308501>
- [24] Balasubramaniam, R., Kumar, A. V. R., and Dillmann, P., "Characterization of Rust on Ancient Indian Iron," *Curr. Sci.*, Vol. 85, No. 11, 2003, pp. 1546–1555, [http://dx.doi.org/10.1016/S0010-938X\(02\)00028-8](http://dx.doi.org/10.1016/S0010-938X(02)00028-8)